

# Hepatic-Specific Disruption of SIRT6 in Mice Results in Fatty Liver Formation Due to Enhanced Glycolysis and Triglyceride Synthesis

Hyun-Seok Kim,<sup>1,4</sup> Cuiying Xiao,<sup>1,4</sup> Rui-Hong Wang,<sup>1</sup> Tyler Lahusen,<sup>1</sup> Xiaoling Xu,<sup>1</sup> Athanassios Vassilopoulos,<sup>1</sup> Guelaguetza Vazquez-Ortiz,<sup>1</sup> Won-Il Jeong,<sup>2,3</sup> Ogyi Park,<sup>2</sup> Sung Hwan Ki,<sup>2</sup> Bin Gao,<sup>2</sup> and Chu-Xia Deng<sup>1,\*</sup>

<sup>1</sup>Genetics of Development and Diseases Branch, National Institute of Diabetes and Digestive and Kidney Diseases

<sup>2</sup>Laboratory of Liver Diseases, National Institute on Alcohol Abuse and Alcoholism  
National Institutes of Health, Bethesda, MD 20892, USA

<sup>3</sup>Present address: Graduate School of Medical Science and Engineering, Korea Advanced Institute of Science and Technology, Daejeon 305-701, Republic of Korea

<sup>4</sup>These authors contributed equally to this work

\*Correspondence: [chuxiad@bdg10.niddk.nih.gov](mailto:chuxiad@bdg10.niddk.nih.gov)

DOI 10.1016/j.cmet.2010.06.009

## SUMMARY

Under various conditions, mammals have the ability to maintain serum glucose concentration within a narrow range. SIRT1 plays an important role in regulating gluconeogenesis and fat metabolism; however, the underlying mechanisms remain elusive. Here, we show that SIRT1 forms a complex with FOXO3a and NRF1 on the SIRT6 promoter and positively regulates expression of SIRT6, which, in turn, negatively regulates glycolysis, triglyceride synthesis, and fat metabolism by deacetylating histone H3 lysine 9 in the promoter of many genes involved in these processes. Liver-specific deletion of SIRT6 in mice causes profound alterations in gene expression, leading to increased glycolysis, triglyceride synthesis, reduced  $\beta$  oxidation, and fatty liver formation. Human fatty liver samples exhibited significantly lower levels of SIRT6 than did normal controls. Thus, SIRT6 plays a critical role in fat metabolism and may serve as a therapeutic target for treating fatty liver disease, the most common cause of liver dysfunction in humans.

## INTRODUCTION

In budding yeast and *Drosophila*, the Sir2 histone deacetylase acts as a chromatin silencer to regulate recombination, genomic stability, and aging (Guarente and Kenyon, 2000). In mammals, seven sirtuin proteins (SIRT1-7) have been found to share homology with Sir2 and are suspected to have some functions similar to those of Sir2 (Finkel et al., 2009; Mantel and Broxmeyer, 2008; Saunders and Verdin, 2007; Vaquero et al., 2007). These proteins are primarily localized in different subcellular compartments, with SIRT1 and SIRT2 both in the nucleus and the cytoplasm; SIRT3, SIRT4, and SIRT5 in the mitochondrion; and SIRT6 and SIRT7 in the nucleus (Blander and Guarente, 2004; Haigis and Guarente, 2006; Saunders and Verdin, 2007). Sirtuins have emerged as broad regulators of many important processes,

including cell fate determination, DNA damage repair, neuronal protection, adaptation to calorie restriction (CR), organ metabolism and function, age-related diseases, and tumorigenesis, although much of the information has come from studies of SIRT1 (Ahn et al., 2008; Deng, 2009; Finkel et al., 2009; Jacobs et al., 2008; Kim et al., 2010; Saunders and Verdin, 2007; Vaquero et al., 2007; Wang et al., 2008a; Wang et al., 2008b).

In response to fasting and CR, SIRT1 is induced, which then interacts with and deacetylates peroxisome proliferator-activated receptor gamma-coactivator-1 $\alpha$  (PGC-1 $\alpha$ ) and controls gluconeogenic and glycolytic pathways in the liver (Rodgers et al., 2005; Rodgers and Puigserver, 2007). For example, it was demonstrated that SIRT1 and the histone acetyltransferase p300 form a fasting-inducible switch that maintains energy balance and regulates hepatic glucose production in mice through sequential induction of CREB regulated transcription coactivator 2 (CRTC2) and PGC-1 $\alpha$ /FOXO1 (Liu et al., 2008). During early fasting, P300 modulates fasting gluconeogenesis through acetylating CRTC2, which protects CRTC2 from ubiquitin-mediated degradation. During late fasting, SIRT2 is induced, and the deacetylation of CRTC2 by SIRT1 promotes ubiquitin-dependent degradation of CRTC2, thereby attenuating the CRTC2-stimulated hepatic glucose production. This switch strongly correlates with a transition from a high level of gluconeogenesis in the early phase of fasting to a lower level of glucose production at a later time. SIRT6 may also play a role in glucose metabolism, because SIRT6 null mice suffer hypoglycemia before they die at 3–4 weeks of age (Mostoslavsky et al., 2006; Zhong et al., 2010). SIRT6 protein expression can be induced by nutritional stress (Kanfi et al., 2008); however, the physiological role of SIRT6 in response to nutritional status and its relationship with SIRT1 remains unclear.

To elucidate the function of SIRT6 and its relationship with SIRT1, we performed an in vitro study to understand the regulation of SIRT6 by SIRT1, generated liver-specific SIRT6 knockout mice, and performed a comprehensive phenotypic analysis in gene expression and acetylation associated with SIRT6 deficiency. Our data revealed that SIRT1 regulates SIRT6 by forming a complex with FOXO3a and NRF1 on the promoter of SIRT6. In turn, SIRT6 deacetylates lysine 9 of histone H3 (H3K9) on the promoters of many genes, which have an essential role in glycolysis and lipid metabolism.

## RESULTS

### SIRT1 Positively Regulates SIRT6

We first investigated the relationship between SIRT1 and SIRT6 in mice under fed, fasted, and re-fed conditions. Analysis of multiple organs revealed increased SIRT1 protein in the brain, liver, white adipose tissue (WAT), and kidney of fasted mice to a varying degree, although SIRT1 mRNA was increased in the brain only (Figures 1A and 1C). In contrast, SIRT6 mRNA and protein were coordinately increased in the brain, WAT, and liver in fasted mice (Figures 1B and 1C). Next, we performed a time-course study in the liver after fasting. We detected a positive correlation of SIRT1 induction and SIRT6 induction, and in addition, we found that the increase in SIRT1 protein occurred earlier than that of SIRT6 (Figure 1D). For example, an obvious increase in SIRT1 occurred at 12 hr and peaked at 18 hr after fasting, whereas a significant increase in SIRT6 was detected at 18 hr. Of note, fasting also induced expression of the gluconeogenic genes *G6Pase* and phosphoenolpyruvate carboxylase 1 (*Pepck*) (Figure 1E) and inhibited expression of glycolytic genes glucokinase (*Gk*) and liver pyruvate kinase (*Lpk*) (Figure 1F). A similar expression pattern of SIRT1 and SIRT6 induction was also detected in cultured primary hepatocytes and hepatoma cell lines in the absence of glucose (see Figures S1A–S1D available with this article online).

To further elucidate the relationship between SIRT1 and SIRT6, we examined SIRT6 expression in the liver of *Sirt1*<sup>-/-</sup> mice (Wang et al., 2008a). Our data revealed that both SIRT6 mRNA and protein were reduced by 50% and failed to be induced by fasting (Figures 1G and 1H). Furthermore, SIRT1 ectopic expression in Hepa1-6 cells induced SIRT6 mRNA in glucose-containing medium, which was further increased in the absence of glucose (Figure 1I). Conversely, siRNA-mediated SIRT1 knockdown blocked SIRT6 induction in the absence or presence of glucose (Figure 1J), indicating that SIRT1 is involved in maintaining SIRT6 expression under the physiological conditions and is required for SIRT6 induction during fasting.

### Regulation of SIRT6 by SIRT1 through NRF1-Binding Sites in the SIRT6 Promoter

To understand the mechanism of SIRT6 induction by SIRT1, we examined the activity of the SIRT6 promoter. Our data using serial deletions of the SIRT6 promoter revealed that a region between 0.17 kb and 0.13 kb was essential for the stimulatory effect by glucose starvation (Figure S2A). Using a software program for candidate transcription factors, we identified two predicted nuclear respiratory factor 1 (NRF1)-binding sites in this region (Figure S2B). Mutation of either site significantly impaired SIRT6 induction in the absence of glucose, whereas mutation of both sites completely blocked the induction (Figure 2A). These data indicate that NRF1-binding sites are involved in the regulation of the SIRT6 promoter by glucose starvation.

NRF1 is a transcription factor, and its expression is regulated by CR (Mahishi and Usdin, 2006; Nisoli et al., 2005). To understand the role of NRF1 in the regulation of SIRT6 expression, we performed both NRF1 overexpression and knockdown experiments. Our data indicate that ectopic expression of NRF1 did not have a significant effect on a SIRT6 promoter

reporter (Figure 2B), whereas RNAi-mediated knockdown of NRF1 blocked the induction of the SIRT6 promoter by glucose starvation (Figure 2C). A similar effect was observed for endogenous SIRT6 mRNA expression (Figures S2C and S2D). The amount of endogenous NRF1 is sufficient to maintain SIRT6 expression either with or without glucose; thus, an increase in NRF1 by ectopic expression does not have additional effects.

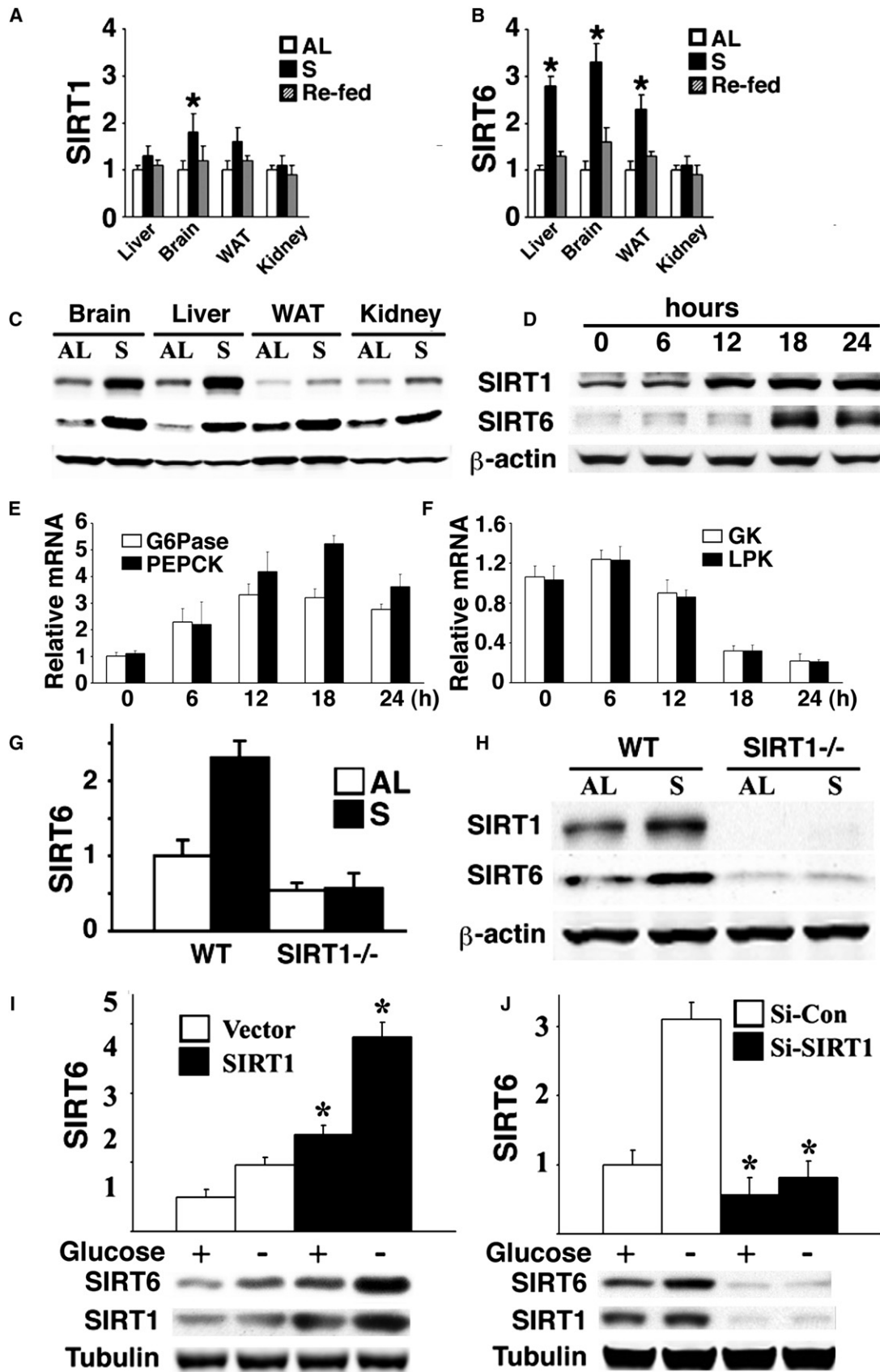
Next, we showed that ectopic expression of SIRT1 increased SIRT6 promoter activity by approximately three-fold, either with or without glucose, and this stimulatory effect was lost when the NRF1-binding sites in the SIRT6 promoter were mutated (Figure 2D). Furthermore, SIRT6 promoter activity induced by the absence of glucose could be blocked by RNAi-mediated knockdown of SIRT1 (Figure 2E). These data suggest that SIRT1 plays an important role in regulating SIRT6 through NRF1-binding sites in the SIRT6 promoter.

### Regulation of SIRT6 by SIRT1, FOXO3a, and NRF1 Protein Complex upon Nutritional Stress

FOXO3a plays an important role in SIRT1 induction by glucose and serum starvation (Nemoto et al., 2004). Therefore, we determined whether FOXO3a is also involved in the regulation of SIRT6 expression. We found that SIRT6 promoter activity was increased four-fold after transfection of a FOXO3a expression vector, compared with a GFP expression vector in the presence of glucose, and that the induction was increased further in the absence of glucose (Figure 2F). Conversely, knockdown of FOXO3a by siRNA significantly reduced SIRT6 promoter activity (Figure 2G). Our analysis of endogenous SIRT6 mRNA (Figure 2H) expression in Hepa1-6 cells confirmed these changes. Thus, both SIRT1 and FOXO3a were capable of regulating the expression of SIRT6 mRNA through the NRF1-binding sites in both fed and fasting conditions.

Next, we studied potential interactions among SIRT1, FOXO3a, and NRF1 in regulating SIRT6 expression. We showed that cotransfection of SIRT1 and FOXO3a enhanced SIRT6 expression, compared with transfection of these genes alone, as revealed by a SIRT6 promoter reporter assay (Figures S3A and S3C) and endogenous SIRT6 gene expression (Figures S3B and S3C) either with or without glucose. We found that, although ectopic overexpression of NRF1 did not have an apparent effect on SIRT6 induction by SIRT1 and/or FOXO3a (data not shown), siRNA-mediated NRF1 knockdown completely blocked such induction (Figure 3A). This finding suggests that the amount of endogenous NRF1 is sufficient for SIRT6 induction by SIRT1 and/or FOXO3a. In addition, FOXO3a knockdown blocked induction of SIRT6 by SIRT1 (Figure S3D) and the absence of SIRT1 blocked induction of SIRT6 by FOXO3a (Figure S3E). Collectively, these data suggest that SIRT1, FOXO3a, and NRF1 might form a complex on the SIRT6 promoter with a defined configuration.

In light of these findings, we examined whether these factors could bind to the SIRT6 promoter using chromatin immunoprecipitation (ChIP) assay. We showed that both SIRT1 and FOXO3a bind to a fragment containing NRF1 sites on the SIRT6 promoter. This binding was enhanced by approximately three-fold in the absence of glucose, whereas the binding of NRF1 was not affected (Figure 3B). Using an oligonucleotide pull-down assay, it was determined that the NRF1-binding sites were critical for



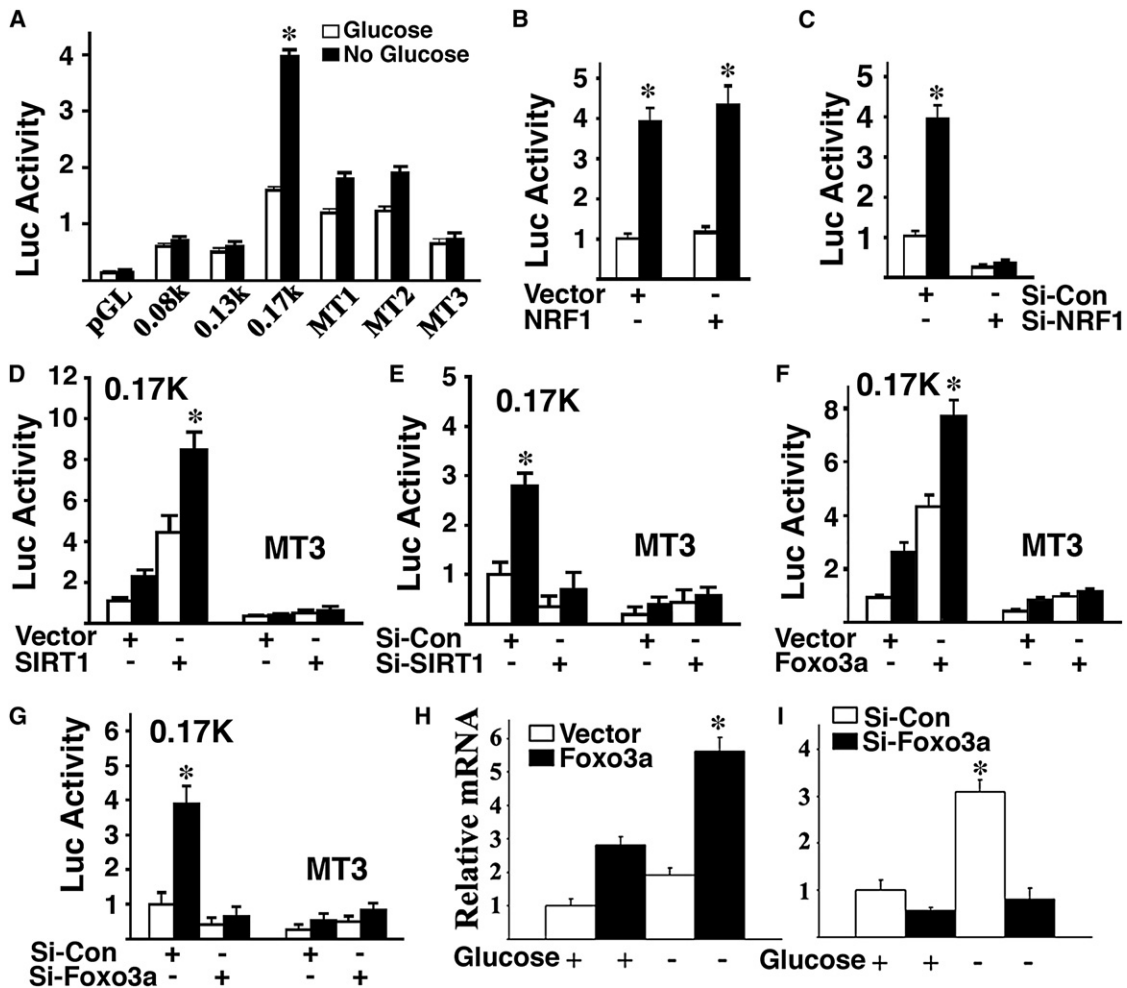


**Figure 2. Regulation of SIRT6 by SIRT1, FOXO3a, and NRF1**

(A) Absence of glucose in Hepa1-6 cells induced luciferase activity of a SIRT6 promoter reporter, whereas mutation of NRF1-binding sites abolished the induction. (B and C) Effect of NRF1 ectopic expression (B) and RNAi-mediated knockdown (C) on a SIRT6 promoter reporter. (D and E) Ectopic expression of SIRT1 increased SIRT6 promoter activity in the presence or absence of glucose (D), whereas mutation of NRF1-binding sites (D), or RNAi-mediated knockdown of SIRT1 (E) abolished the induction. (F and G) Ectopic expression of FOXO3a increased SIRT6 promoter activity in the presence or absence of glucose (F), whereas RNAi-mediated knockdown of FOXO3a inhibits it (G). (H and I) Absence of glucose induces expression of SIRT6 mRNA, which is further increased by overexpression of FOXO3a (H), whereas RNAi-mediated knockdown of FOXO3a abolished the induction (I).

complex formation (Figure S3F). We further showed that siRNA-mediated knockdown of either FOXO3a or SIRT1 (Figures S3G and S3H) blocked interaction of these factors at the NRF1 sites, whereas knockdown of either of them did not affect the binding of NRF1 to the SIRT6 promoter (bottom lane of Figures S3G and S3H). These data suggest that both SIRT1 and FOXO3a bind

cooperatively to the SIRT6 promoter, whereas binding of NRF1 to the SIRT6 promoter does not require SIRT1 or FOXO3a.

Next, we performed experiments to examine protein-protein interaction. We showed that all three proteins (SIRT1, FOXO3a, and NRF1) interacted with each other in cells in the presence of glucose, whereas the interaction was markedly enhanced in

**Figure 1. Regulation of SIRT1 and SIRT6 Expression by Nutrient Deprivation**

(A–C) Levels of mRNA (A and B) and protein (C) of SIRT1 and SIRT6 in multiple organs of mice under fed ad libitum (AL), starved (S), or re-fed for 24 hr. (D–F) Levels of SIRT1 and SIRT6 protein (D), G6Pase and PEPCK mRNA (E), and GK and LPK mRNA (F) in the liver of wild-type mice during a time course of fasting. (G and H) Levels of SIRT6 mRNA revealed by Real-Time RT-PCR (G) and protein (H) in the liver from wild-type and *Sirt1*<sup>-/-</sup> mice. (I and J) Overexpression of SIRT1 increased endogenous SIRT6 in the presence and absence of glucose (I), whereas RNAi-mediated knockdown of SIRT1 blocked SIRT6 induction in the absence of glucose (J) revealed by real-time PCR. \* p < 0.05, by Student's t test in all figures.

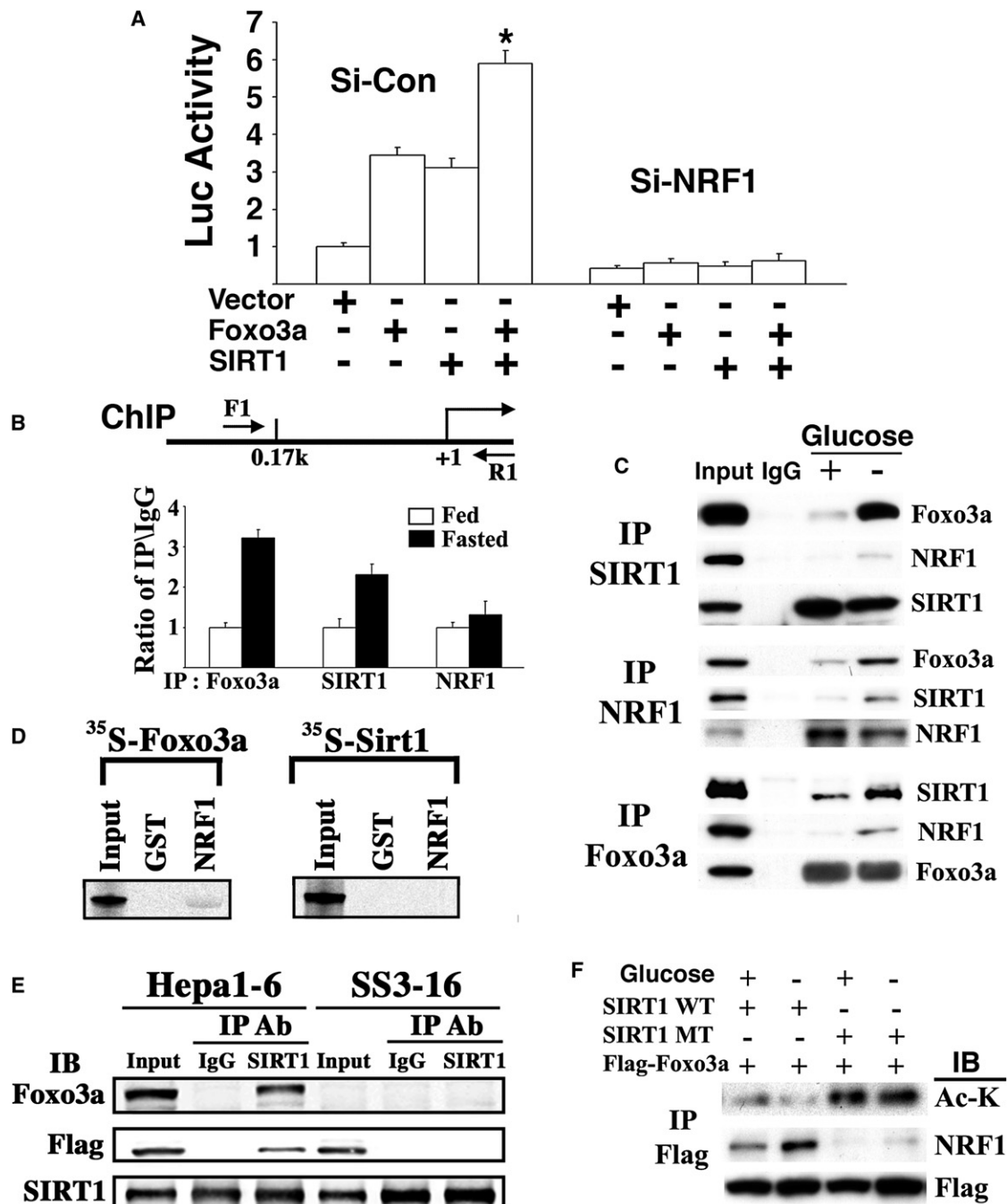


**Figure 3. SIRT1, FOXO3a, and NRF1 Form a Protein Complex on the NRF1-Binding Sites of the SIRT6 Promoter**

(A) Expression of SIRT1 and FOXO3a synergistically activated a SIRT6 promoter reporter, which is blocked by siRNA specific to NRF1. (B) Binding of NRF1, SIRT1, and FOXO3a to the SIRT6 promoter in the presence or absence of glucose, as revealed by ChIP assay. (C) Interaction of FOXO3a, SIRT1, and NRF1 in cultured cells in either the presence or absence of glucose, as revealed by immunoprecipitation (IP). (D) Pull-down of <sup>35</sup>S-FOXO3a, but not <sup>35</sup>S-SIRT1, by GST tagged-NRF1. (E) SIRT1 pulls down both FOXO3a and NRF1 in Hepa1-6 cells. However, SIRT1 could not pull down NRF1 in Hepa1-6 cells carrying a stably transfected shRNA for FOXO3a (SS3-16). (F) Wild-type SIRT1 deacetylates FOXO3a, which is enhanced in the absence of glucose in Hepa1-6 cells, and the deacetylated form of FOXO3a interacts more abundantly with NRF1.

the absence of glucose (Figure 3C). Thus, glucose deprivation enhanced the formation of a SIRT1-FOXO3a-NRF1 (SFN) protein complex on the SIRT6 promoter that is responsible for the induction of SIRT6 expression. Notably, our study revealed that GST-tagged NRF1 only pulled down <sup>35</sup>S-FOXO3a but not <sup>35</sup>S-SIRT1 (Figure 3D). Furthermore, shRNA-mediated

knockdown of FOXO3a in Hepa1-6 cells blocked the interaction between SIRT1 and NRF1 (Figure 3E). Altogether, these data indicate that NRF1 binds directly to the SIRT6 promoter irrespective of glucose concentration, whereas SIRT1 binds to NRF1 through FOXO3a.

Previous studies have shown that SIRT1 binds and deacetylates FOXO3a (Brunet et al., 2004; Motta et al., 2004). Because we found that expression of a dominant-negative mutant form of SIRT1—SIRT1 (HY), which lacks deacetylase activity—blocked the induction of SIRT6 by SIRT1 and/or FOXO3a (Figures S3A–S3C), we investigated whether the acetylation status of FOXO3a could affect its interaction with NRF1. Our data showed that the presence of wild-type SIRT1 repressed FOXO3a acetylation as compared with expression of the mutant SIRT1 (HY) (Figure 3F). The absence of glucose further decreased FOXO3a acetylation (compare the first 2 lanes in Figure 3F), whereas no reduction of FOXO3a acetylation was observed in the SIRT1 (HY) transfected cells (compare the last 2 lanes in Figure 3F). The data also revealed increased interaction between FOXO3a with NRF1 in the cells with expression of wild-type SIRT1, compared with cells with mutant SIRT1 (Figure 3F). A stronger band was also detected in the wild-type SIRT1-expressed cells in the absence of glucose (Figure 3F). Altogether, these data indicate that the absence of glucose enhances the interaction between SIRT1 and FOXO3a, as well as the deacetylation of FOXO3a. Deacetylated FOXO3a has higher binding affinity for NRF1, resulting in the increased quantity of SFN complex on the SIRT6 promoter that accounts for the increased expression of SIRT6 upon nutritional stress.

### Liver-Specific Knockout of SIRT6 Results in Fatty Liver

The observation that up-regulation of SIRT6 through the SFN complex under fasting conditions suggests that SIRT6 plays a role in glucose metabolism in the liver. Because *Sirt6*<sup>-/-</sup> mice die shortly after weaning (Mostoslavsky et al., 2006), we generated liver-specific SIRT6 knockout mouse using albumin-Cre (Yakar et al., 1999) to overcome this early postnatal lethality (Figure S4). *Sirt6*<sup>Co/Co</sup>; *Alb-Cre* mice appeared morphologically normal and displayed comparable levels of blood glucose at one month of age (data not shown), suggesting that the hypoglycemia and lethal phenotype observed in *Sirt6*<sup>-/-</sup> mice (Mostoslavsky et al., 2006) are not caused by the lack of SIRT6 in the liver. Consistent with this observation, our study using older mice ranging in age from 1 to 8 months also failed to reveal a significant difference in blood glucose between SIRT6 mutant and control mice after feeding (data not shown). Of note, our analysis of older *Sirt6*<sup>Co/Co</sup>; *Alb-Cre* mice (≥8 months of age) revealed slightly increased blood glucose (Figure 4A). The mutant mice also exhibited slightly higher levels of glucose in the glucose tolerance test (GTT) (Figure 4B) and insulin tolerance test (ITT) (Figure 4C), although glucose level did not reach a significant level at most time points. The elevation in glucose might be caused by an increase in hepatic glucose production. However, additional studies on hepatic gluconeogenesis, including the pyruvate tolerance test and clamp analysis, failed to detect increased hepatic gluconeogenesis in these mutant mice (data not shown), suggesting that this phenotype might not be a direct consequence of SIRT6 deficiency in the liver.

*Sirt6*<sup>Co/Co</sup>; *Alb-Cre* mice gradually increased in body weight beginning at 5 months of age, although such an increase did not reach a statistically significant level (Figure 4D). There was no significant difference in body fat, plasma concentration of lipids and insulin, as well as insulin signaling between SIRT6 mutant and wild-type mice (data not shown). However, our examination revealed that 43% (3/7) of *Sirt6*<sup>Co/Co</sup>; *Alb-Cre* mice started to develop fatty liver at 5–6 months of age, and reached 90% (9/10) from 7.5–13 months of age, as revealed by increased liver weight (Figure 4E), hepatic triglyceride (TG) (Figure 4F), gross morphology (Figures 4G and 4H), histopathology (Figures 4I and 4J), and Oil Red O staining (Figures 4K and 4L). In contrast, only 12% (2/17) of control animals exhibited mild fatty liver from 5–13 months of age.

Theoretically, an increase in hepatic TG could be caused by reduced VLDL export, increased TG synthesis, and/or increased TG uptake. Our experiments indicated that SIRT6 mutant mice had a slightly higher rate of TG secretion from the liver to the blood compared with wild-type mice (Figure 4M). To measure TG synthesis, we cultured primary hepatocytes in the presence of oleic acid, which stimulates TG synthesis, with or without <sup>3</sup>H-Palmitate. The data revealed significantly higher levels of TG in the mutant cells than controls in both conditions (Figures 4N and 4O). These data suggest that the increased hepatic TG in SIRT6 mutant mice may be caused by increased TG synthesis, rather than reduced TG secretion.

### SIRT6 Deficiency Causes Altered Expression of Genes Involved in Glycolysis and Lipid Metabolism

Fatty liver occurs at a high frequency in humans and may be caused by altered signaling in multiple biological pathways, including glycolysis, fatty acid uptake and synthesis, and TG synthesis (Postic and Girard, 2008). We observed an inverse correlation in gene expression between SIRT6 and glycolytic genes, GK and Lpk (Figures 1D and 1F) during the course of fasting, so we first investigated the impact of SIRT6 deficiency on glycolysis. Our analysis of the fatty liver of 8–9-month old mutant mice revealed significantly increased expression of both *Gk* and *Lpk* (Figure 5A). To investigate whether this change in gene expression is directly related to a SIRT6 deficiency, we analyzed the liver of mutant mice at 2–3 months of age prior to fatty liver development. We found that SIRT6 deficiency resulted in approximately a two-fold increase in *Gk* mRNA, compared with wild-type mice (Figure 5B). Upon fasting, *Gk* mRNA level was reduced to 20% of the fed level in wild-type mice; however, in SIRT6 mutant mice, this reduction was significantly attenuated, leading to about six-fold higher *Gk* mRNA (Figure 5B). Significantly higher levels of GK protein (Figure 5C) and enzymatic activity (Figure 5D) were observed in the SIRT6 mutant liver than control liver in both fed and fasting conditions. A similar increase in *Lpk* mRNA was also observed in the liver of *Sirt6*<sup>Co/Co</sup>; *Alb-Cre* mutants, compared with wild-type mice (Figure 5B). These data indicate that SIRT6 deficiency increases glycolysis under both fed and fasting conditions.

Next, we checked the expression level of lipid metabolism-related genes. The liver of 2–3-month-old *Sirt6*<sup>Co/Co</sup>; *Alb-Cre* mice exhibited moderate, yet statistically significant, increased levels of fatty acid translocase (*Fat*), which uptakes long chain fatty acid from blood, compared with the control mice in both

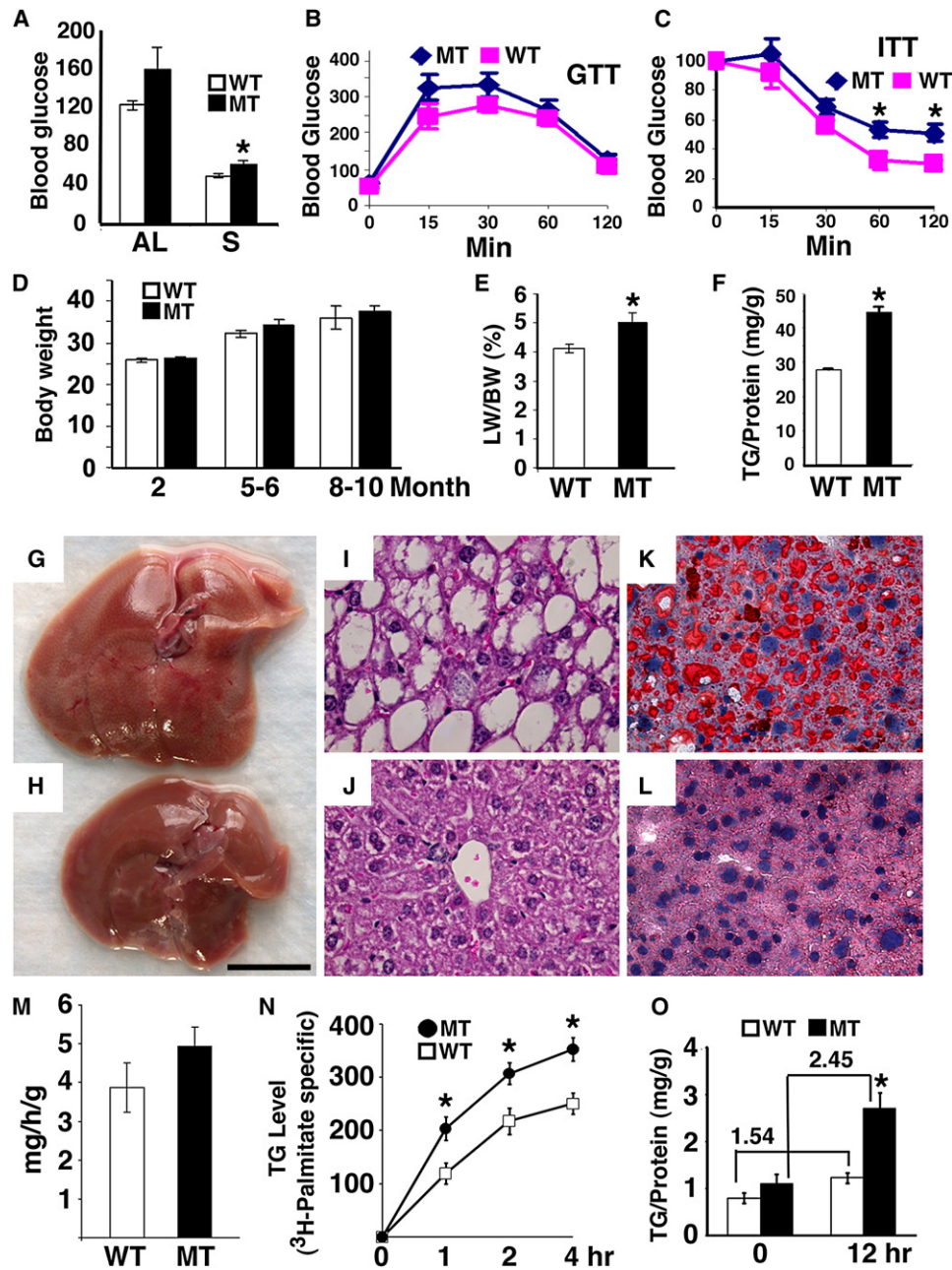


**Figure 4. Phenotypic Analysis of Mice Carrying a Liver-Specific Knockout of SIRT6**

(A) Blood glucose level (mg/dL) of 8–9-month-old SIRT6 MT and WT mice under fed or 24 hr fasting condition.

(B) Glucose tolerance test. Mutant mice had a slightly higher, but not significantly different glucose levels at 15 and 30 min than wild-type mice.

(C) Insulin tolerance test expressed as percentage of basal glucose level. We have also measured glucose value in the area under the curve (AUC) for both GTT and ITT, and no difference was found between wild-type and mutant mice.

(D) Body weight (grams) of SIRT6 mice at 2 months (WT, 17; and MT, 15), at 5–6 months (WT, 18; and MT, 15), and at 8–10 months (WT, 15; and MT, 22).

(E and F) Percentage of liver weight/body weight (E) and hepatic TG levels (F) of 8–9-month-old SIRT6 MT and WT mice.

(G–L) Morphology (G and H), H&E sections (I and J) and Oil Red O staining (K and L) of livers from MT (G, I, and K) and WT (H, J, and L) mice. Bar in (G and H) is 1 cm. At least 6 pairs of mice were analyzed in each experiment.

(M) TG secretion rate to plasma (mg/hour/gram of liver).

(N and O) TG content in primary hepatocytes measured by <sup>3</sup>H-palmitate incorporation (N) and TG level (O) at different times. In panel (O), TG production increases 1.54 fold in wild-type cells and 2.45 fold in mutant cells from 0 hr to 12 hr, respectively. This increase is statistically significant with  $p < 0.04$ .

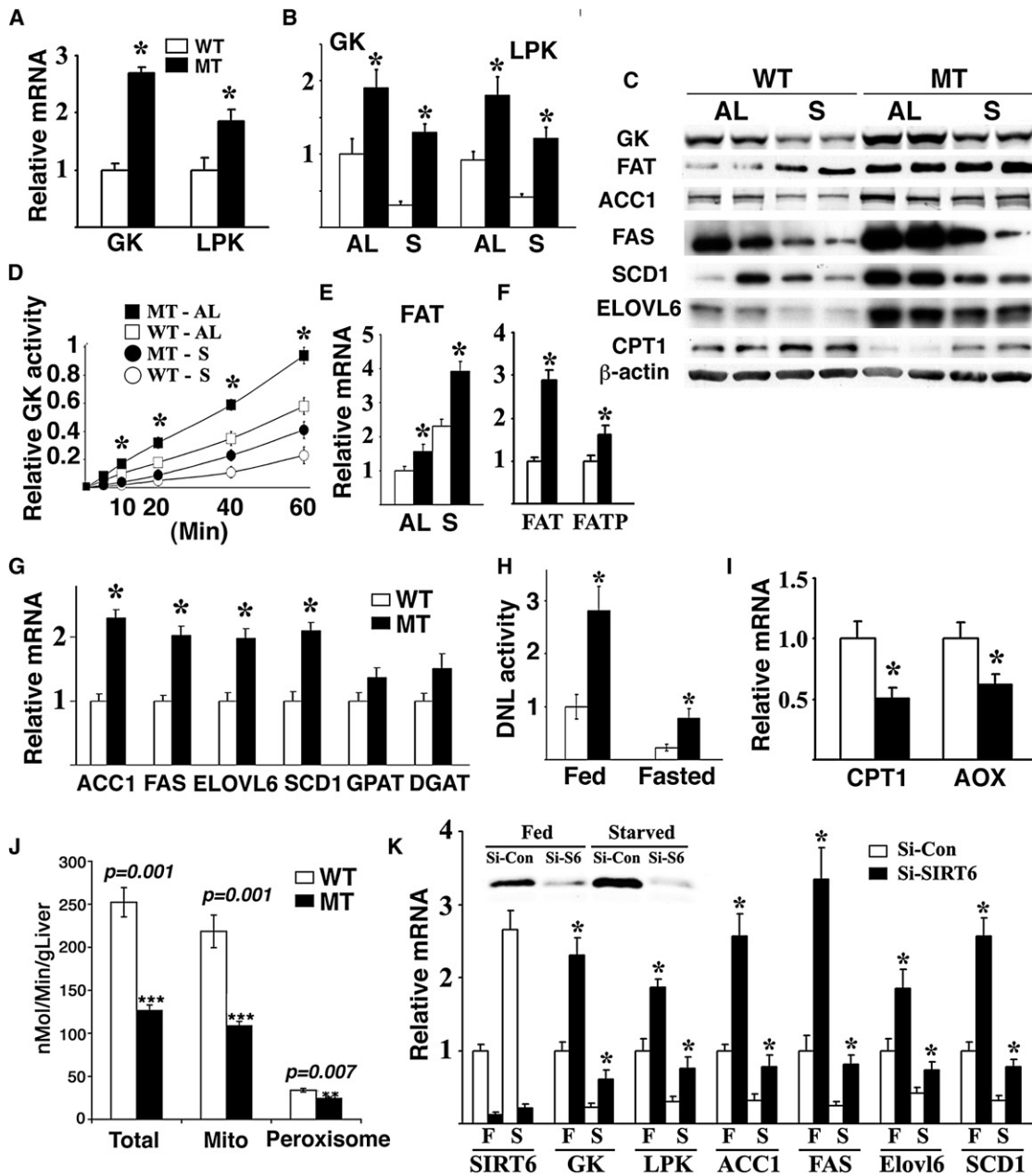


**Figure 5. SIRT6 Regulates the Expression of Genes Related to Glycolysis and Lipid Metabolism**

(A and B) mRNA levels of GK and LPK in the liver of WT and MT mice at 8–9 months (A) and at 2–3 months (B) under fed ad libitum (AL) or 24 hr starvation (S) detected by using real-time RT-PCR.

(C) Protein expression of genes involved in glycolysis and lipid metabolism.

(D) GK enzymatic activity in the liver of WT and MT mice.

(E–G) mRNA levels of FAT and FATP (E and F) and several genes involved in TG synthesis in the liver (G). Mice used in panels (F and G) were 8–9 months old, and in panels (C–E) were 2–3 months old. At least 5 pairs of mice were used for each experiment.

(H) De novo lipogenesis activity in the primary hepatocytes under fed or fasted condition.

(I and J) Absence of SIRT6 decreased the expression levels of genes involved in  $\beta$  oxidation revealed by real-time RT-PCR (I) and fatty acid  $\beta$  oxidation revealed by enzymatic activity (J).

(K) Gene expression in primary hepatocytes upon acute knockdown of SIRT6 for 36 hr revealed by real-time PCR. Abbreviations for genes that are not mentioned in the text: ACC1, acetyl-CoA carboxylase-1; Elov16, long-chain elongase; FAS, fatty acid synthase; GPAT, mitochondrial glycerol 3-phosphate acyltransferase; and SCD1, stearyl-CoA desaturase-1.



fed and fasting conditions (Figures 5C and 5E). *Fat* transcripts increased about three-fold in 8–9-month-old mutant mice, compared with controls (Figure 5F). *Sirt6<sup>Co/Co</sup>;Alb-Cre* mice also exhibited increased mRNA of fatty acid transport protein (*Fatp*) (Figure 5F) and of several genes involved in lipogenesis, fatty acid elongation, and desaturation (Figures 5C and 5G). Consistent with the increased expression of lipogenic genes, about a three-fold increase in lipid production was detected in the primary hepatocytes of *Sirt6<sup>Co/Co</sup>;Alb-Cre* mice than that of WT mice under both fed and fasting conditions (Figure 5H). SIRT6 mutant liver also exhibited significantly decreased levels of liver–carnitine palmitoyltransferase I (*L-cpt1*) and acyl-Coenzyme A oxidase 1, palmitoyl (*Aox*) (Figures 5C and 5I), and lower levels of fatty acid  $\beta$  oxidation (Figure 5J), whereas expression of genes upstream of TG synthesis or involved in TG secretion were not affected (data not shown).

These data suggest that SIRT6 may regulate expression of many genes involved in various steps of glycolysis and lipid metabolism. To rule out a possibility that the expression change of these genes is secondary to a long-term loss of SIRT6, we performed acute knockdown of SIRT6 in primary hepatocytes. Our data showed that SIRT6 knockdown caused an increased expression of these genes (Figure 5K). Conversely, infection of a SIRT6 expression vector using a lentiviral system into these cells resulted in a significant reduction in expression of these genes than the control vector under fed and fasting conditions (Figure S5A). These data provide convincing evidence that SIRT6 inhibits the expression of these genes.

#### SIRT6 Binds and Deacetylates H3K9 in the Promoters of Genes Involved in Glycolysis and Lipid Metabolism

First, we investigated the mechanism underlying expression changes of these genes that are associated with SIRT6 deficiency. We found that levels of acetylated H3K9 (AcH3K9) were significantly higher in the liver of SIRT6 mutant mice than controls (Figure 6A). Furthermore, fasting significantly reduced AcH3K9 in the liver of wild-type mice, but SIRT6 deficiency blocked such a reduction. A similar pattern of AcH3K9 levels was observed in SIRT6 mutant mouse embryonic fibroblast cells (MEFs), whereas modification of several other lysines in H3, and K16 of H4 was not affected (data not shown). Furthermore, primary hepatocytes that overexpressed FLAG-SIRT6 exhibited reduced levels of AcH3K9 (Figure 6B). These data suggest that SIRT6 plays a specific role in deacetylation of AcH3K9 in both fed and fasting conditions.

Next, we investigated whether altered AcH3K9 could be detected in the promoter of the genes that were studied earlier. ChIP assay of the proximal region revealed increased levels of AcH3K9 in the promoters of *Gk*, *Lpk*, *Fat*, *ACC1*, *FAS*, *Elovl6*, and *SCD1* in the liver of SIRT6 mutant mice (Figures 6C–6G). There was no obvious change in the promoters of GPAT and DGAT, which is consistent with their expression (Figure S5B). To confirm whether SIRT6 can recruit and deacetylate H3K9 on these promoters, we performed ChIP assay after infection of a FLAG-SIRT6 vector into primary hepatocytes that were cultured under fed and fasted condition. SIRT6-infected cells had a lower level of AcH3K9 in the proximal promoter region of these genes than cells infected with vector control, but no differ-

ence was found in the coding or intron region of those genes (Figure S5C). We further investigated whether SIRT6 could bind to the promoter of these genes. ChIP analysis showed that SIRT6 was recruited to the proximal region but not to the coding/intron region of those genes (Figure S5D, and data not shown). Furthermore, ChIP analysis on endogenous genes also indicated that SIRT6 occupies the promoters of these genes (Figure 6H).

In addition, we analyzed the changes in gene expression in WT and SIRT6 mutant livers at both 2 and 8 months of age by microarray analysis and observed that expression of many genes involved in lipid and carbohydrate metabolism were altered Table S1 and GSE21965. The gene change involved in lipid metabolism was consistent with mRNA changes we detected by real-time RT PCR.

Finally, we reintroduced SIRT6 to the liver using a lentiviral-mediated approach. The expression of SIRT6 in SIRT6 mutant liver significantly reversed increased levels of AcH3K9 (Figure 6I) and increased gene expression (Figure 6J), yielding strong evidence that the increased AcH3K9 and altered gene expression is a direct consequence of SIRT6 mutation. Of note, this short-term SIRT6 expression did not have an obvious effect on the fatty liver phenotype, which may reflect a view that the formation of fatty liver is a long process in the SIRT6 mutant liver. Altogether, these data indicate that SIRT6 binds and deacetylates AcH3K9 in the promoter of many genes that are involved in glucose and lipid metabolism, and SIRT6 deficiency resulted in altered expression of these genes, which ultimately led to fatty liver in the mutant mice.

#### Reduced Expression of SIRT1 and SIRT6 in Human Fatty Liver Samples

It has been shown that hepatocyte-specific deletion of SIRT1 resulted in fatty liver in mice (Purushotham et al., 2009) and that expression of SIRT1 was reduced in nonalcoholic fatty liver induced by high-fat diet in rats (Deng et al., 2007). These findings prompted us to examine expression of SIRT1 and SIRT6 in human fatty liver. Our data revealed a significant reduction of both SIRT1 and SIRT6 in human fatty liver samples, compared with normal controls (Figure 7A). The fatty livers also exhibited significantly increased mRNA of *GK* and *LPK* (Figure 7B). These data, combined with findings that SIRT1 regulates SIRT6 and that liver-specific deletion of SIRT6 in mice causes fatty liver, implicate an inhibitory role of SIRT6 in human fatty liver formation.

#### DISCUSSION

In this study, we showed that nutrient deprivation induces expression of both SIRT1 and SIRT6. Although it has been shown that nutritional stress induces SIRT1 through p53 and FOXO3a (Nemoto et al., 2004), our data indicate that the induction of SIRT6 requires SIRT1, because the absence of SIRT1 blocked SIRT6 induction. In addition, we showed that, upon nutritional stress, SIRT1 deacetylates FOXO3a, which subsequently enhances the formation of a SIRT1/FOXO3a/NRF1 (SFN) protein complex on the promoter of SIRT6 that positively regulates SIRT6 expression. Thus, our study reveals for the first time, to our knowledge, that SIRT1 regulates another sirtuin family member through interaction with other transcription factors.

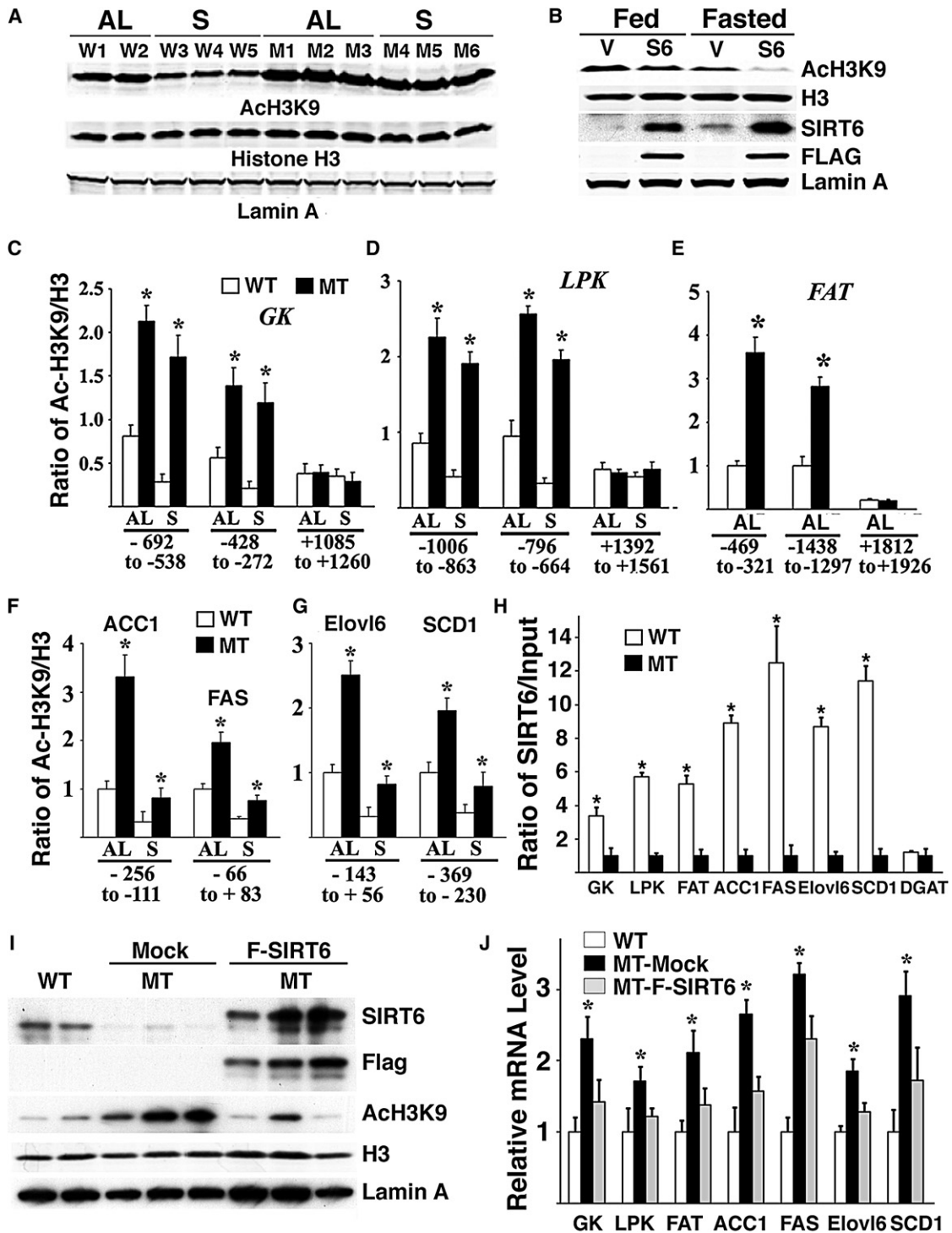


**Figure 6. SIRT6 Is Recruited to and Deacetylates H3K9 in the Promoter of Many Genes**

(A) Western blot analysis of nuclear extracts prepared from the liver of WT and MT mice under fed (AL) or 24 hr starvation (S). (B) Western blot analysis of nuclear extracts prepared from primary hepatocytes infected with pCDH-FLAG-SIRT6 or vector control under fed or fasting condition. (C–G) ChIP analysis showing the acetylation pattern of H3K9 (C–G) in the promoter of several genes in samples extracted from the liver of WT and MT mice. Four fragments (two in promoter region and two in exon/intron) for each gene were analyzed, and, in all cases, the absence of SIRT6 increased acetylation in the promoter, but not in the exon/intron region (some data not shown). (H) ChIP analysis showing the binding of SIRT6 to the promoter of several genes in samples extracted from the liver of WT and MT mice. (I and J) Expression of Flag-tagged SIRT6 in SIRT6 mutant liver mediated by injection of lentivirus carrying Flag-tagged SIRT6 significantly reversed increased levels of AcH3K9 (I) and gene expression (J). At least three pairs of SIRT6 mutant and control mice were used for each experiment.

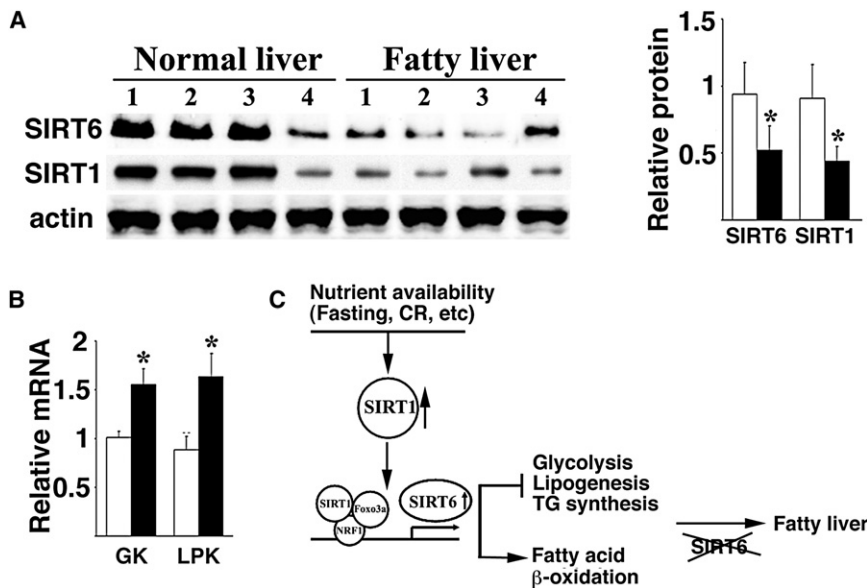


**Figure 7. Reduced Levels of SIRT1 and SIRT6 and Increased Levels of GK and LPK in Human Fatty Liver Samples**

(A) Western blot analysis of protein levels of SIRT1 and SIRT6 in fatty liver samples. Quantification of gel intensity of eight normal livers and eight non-alcoholic fatty livers was shown in right.

(B) mRNA levels of GK and LPK are revealed by real-time RT-PCR in these samples. The fatty livers and controls were provided by the Liver Tissues Procurement and Distribution System (University of Minnesota).

(C) An integrated model for functions of SIRT6 in inhibiting fatty liver formation through regulation of glycolysis and lipid metabolism. SIRT6 deficiency, consequently, results in fatty liver formation.

After bypassing the early postweaning lethality associated with SIRT6 deficiency (Mostoslavsky et al., 2006) using a Cre-loxP-mediated liver specific knockout, we demonstrated that SIRT6 negatively regulates the glycolytic genes, *Gk* and *Lpk*, under both fed and fasting conditions. A previous study indicated that SIRT1 interacts with and deacetylates PGC-1 $\alpha$  and controls gluconeogenic and glycolytic pathways in the liver (Rodgers et al., 2005). Our data indicate that the absence of SIRT6 does not affect expression of *Pgc1 $\alpha$*  and its downstream gene *Pepck*. It also did not affect blood glucose level under fed condition, although a small, yet statistically significant, increase in fasting glucose was observed in *Sirt6<sup>Co/Co</sup>; Alb-Cre* mice 8 months old and older. Thus, SIRT6 mediates a part of SIRT1 function and plays an essential role in glycolysis. In the SIRT6 liver-specific mutant mice, increased glycolysis eventually affected the health of mutant mice as the result of an imbalance in glucose metabolism.

An important finding is that the absence of SIRT6 results in accumulation of TG, which is associated with fatty liver (den Boer et al., 2004; Postic and Girard, 2008). Our data demonstrated that SIRT6 deficiency resulted in increased expression of genes responsible for hepatic long-chain fatty acid uptake and reduced expression of genes for  $\beta$  oxidation. SIRT6 deficiency also increased expression of several genes involved in multiple steps of TG synthesis, whereas expression of genes upstream of TG synthesis and TG secretion were not affected. Increased TG synthesis was also observed in SIRT6 mutant primary hepatocytes, compared with WT hepatocytes, when cultured in vitro. These data suggest that SIRT6 serves as a negative regulator of TG synthesis. Thus, the combined effect of SIRT6 deficiency in the liver causes increased glycolysis, elevated uptake of long chain fatty acid, reduced fat acid  $\beta$  oxidation, and increased TG synthesis and lipogenesis, eventually leading to fatty liver formation (Figure 7C).

It was reported that SIRT6 modulates telomeric chromatin and expression of downstream genes in the NF- $\kappa$ B signaling

response to cell-cycle arrest, suggesting a possible mechanism by which SIRT6 promotes genomic stability (Michishita et al., 2009; Yang et al., 2009). Combined with the early postweaning lethality associated with SIRT6 deficiency, these data underscore important functions of SIRT6 in many biological processes, including DNA damage repair, telomeric chromatin integrity, glucose uptake, and aging through its deacetylase activity and/or ADP-ribosyltransferase activity (Liszt et al., 2005; Lombard et al., 2008; Michishita et al., 2008; Mostoslavsky et al., 2006; Zhong et al., 2010). In this study, although we tried to dissect the complexity of SIRT6 function by specifically deleting SIRT6 in the liver and studying its effects on deacetylation of H3K9 in the promoters of many genes that play a role in glycolysis and lipid metabolism, it is possible that the absence of SIRT6 could still have some effects on many other processes, as revealed by earlier studies. For example, our analysis confirmed that SIRT6 deacetylates H3K56 in DNA isolated from the liver at the global level, but the biological relevance of this modification in metabolism is not clear and will be an interesting topic for future investigation. In addition, our microarray analysis of the liver revealed altered expression of many genes involved in multiple biological processes (Table S1). Although many of the changes can be secondary, some others may be directly linked to SIRT6 mutation, and their impact on histopathological onset and development should be carefully investigated in future studies.

The findings delineated herein have important clinical significance because fatty liver disease is the most common cause of liver dysfunction worldwide (Ahmed and Byrne, 2009; Rogers et al., 2008). We found that human fatty livers exhibited lower levels of SIRT6, compared with normal controls. In light of this finding, SIRT6 mutant and control mice could be used as a model in chemical screens for SIRT6 activators and TG synthesis inhibitors, which may be beneficial for the prevention and/or therapeutic treatment of fatty liver in affected individuals in the near future.

## EXPERIMENTAL PROCEDURES

### Mating and Genotyping Mice

Chimeric mice were mated with NIH Black Swiss females (Taconic) to screen for germline transformation. Male mice bearing germline transmission were mated with female FVB EII-Cre mice (Lakso et al., 1996) to generate conditional *SIRT6* mice, according to a procedure described elsewhere (Xu et al., 2001). Mice carrying a *SIRT6* conditional allele were genotyped by PCR using primers P1 (5' GCTAATGGGAACGAGACCAA 3') and P2 (5' ACCCAC CTCTCTCCCCATAAA 3'). This primer pair flanks the *LoxP* insertion site in intron 1 and amplifies a 390-bp fragment from the wild-type *Sirt6* gene and 444 bp from the conditional allele. The recombination allele of *SIRT6* is amplified using primers P1 and P3 (5'-GCGTCCACTTCTCTTCTCTG-3'), which produces a fragment of 524 bp. All experiments were approved by the Animal Care and Use Committee of the National Institute of Diabetes, Digestive and Kidney Diseases (ACUC, NIDDK).

### Lentivirus Injection into Mouse Tail Vein

To prepare lentiviral particles for injection, 293 T cells were transfected with PsPAX2, VSV-G, and either pCDH or pCDH-mSIRT6 Flag. After 2 days, 30 ml of virus-containing media was collected and concentrated by ultracentrifugation. Mice were then injected twice (once per week) by tail-vein injection with 100  $\mu$ l of concentrated virus. Mouse liver was then harvested for analysis after 2 weeks.

### Determination of Hepatic Triglyceride Secretion

We used a protocol modified from Tietge et al. (1999). Briefly, mice were injected with 100  $\mu$ l of 10% Tyloxapol (Triton WR1339, which inhibits all lipoprotein lipases and therefore clearance of TG from the blood) per animal by IV injection, and blood was collected to check TG at 0 min, 1 hr, and 2 hr. Plasma was separated and assayed for triglycerides. TG secretion rates were expressed as milligram per kilogram per hr after normalizing with their liver weight.

### Triglyceride Assay in the Liver and Cultured Hepatocytes

The triglyceride level of liver was measured as described elsewhere (Jeong et al., 2008; You et al., 2004). Liver extracts were prepared by homogenization in 0.25% sucrose with 1 mmol/L EDTA, and lipids were extracted using chloroform/methanol (2:1 v/v) and suspended with 5% fatty acid-free BSA. Triglyceride level was measured using triglyceride assay reagents (Sigma Chemical Co.). For measuring triglyceride synthesis in cultured primary hepatocytes, freshly isolated hepatocytes from 5-week-old WT and MT mice were cultured for 24 hr with normal media (DMEM with 10% FBS) in the presence or absence of oleic acid (500 mM). Quantitative estimation of hepatic triglyceride accumulation was performed by extraction of hepatic lipids from cell homogenates using chloroform/methanol (2:1) and enzymatic assay of triglyceride mass using EnzyChrom™ Triglyceride assay kit (Bioassay Systems).

### Glucokinase Assay

Glucokinase activity was determined by an enzyme-linked assay based on the NADP<sup>+</sup>/NADPH ratio (Gonzali et al., 2001). The proteins extracted from mouse liver were incubated in the buffer with 12 mM MgCl<sub>2</sub>, 6.5 mM ATP, 1 mM DTT, 0.9 mM NADP<sup>+</sup>, 1 IU/ml glucose-6-phosphate dehydrogenase (Sigma), 45 mM glucose, and 32 mM sodium-HEPES buffer (pH 7.6) at 22°C, and then the absorbance was measured at 340 nm for several time points.

### De Novo Lipogenesis Assay

Primary hepatocytes were cultured with 10% DMEM with insulin (100 nM) and dexamethasone (1  $\mu$ M) overnight and then were incubated with 74 KBq/ml (2-<sup>14</sup>C) sodium acetate (2.07 GBq/mmol; GE Healthcare Inc.) for 1 hr. The cells were lysed with 1 N NaOH and were acidified (Harada et al., 2007). Then, the lipids were extracted with petroleum ether, and radioactivity was measured by liquid scintillation counter (Beckman Inc.).

### Fatty Acid $\beta$ Oxidation Activity

Fatty acid  $\beta$  oxidation activity was measured by the method of Shindo et al. (1978), with some modifications. Briefly, 0.3 g of fresh livers were homogenized in 1.2 ml of 0.25 M sucrose containing 1 mM EDTA in a Potter-Elvehjem

homogenizer using a tight-fitting teflon pestle. Approximately 500  $\mu$ g of homogenate (no centrifugation) was incubated with the assay medium in 0.2 ml of 150 mM potassium chloride, 10 mM HEPES (pH 7.2), 0.1 mM EDTA, 1 mM potassium phosphate buffer (pH 7.2), 5 mM Tris malonate, 10 mM magnesium chloride, 1 mM carnitine, 0.15% bovine serum albumin, 5 mM ATP, and 50  $\mu$ M C14-palmitic acid (5.0  $\times$  10<sup>4</sup> cpm of radioactive substrate). The reaction was run for 30 min at 25°C and was stopped by the addition of 0.2 ml of 0.6 N perchloric acid. The mixture was centrifuged at 2,000  $\times$  g for 10 min, and the unmetabolized fatty acids were removed by three extractions using 2 ml of n-hexane. Radioactive degradation products in the water phase were counted. In some experiments, 2 mM potassium cyanide was added to the incubation mixture to inhibit mitochondrial  $\beta$  oxidation activity. Fatty acid  $\beta$  oxidation activity was expressed as nanomoles per minute per gram of liver.

### Human Liver Clinical Samples

All of these nonalcoholic fatty liver samples were collected from donor livers or recipient livers during liver transplantation from the Liver Tissue Procurement and Distribution System, University of Minnesota. These samples are case 647, 50 years old, female white, AST 13 U/L; case 753, 16 years old, male, AST 43 U/L; case 801, 44 years old, female white, AST 46; case 935, 60 years old, female, AST 30; case 970, 62 years old, female, AST 25; case 1075, 56 years old, male, AST 77; case 1098, 59 years old, female, AST 64; and case 1095, 61 years old, female, AST 59. Normal healthy liver samples were also provided by the Liver Tissue Procurement and Distribution System, and were collected from the part of donor livers that was not used for transplantation. All of samples were collected by quickly freezing in liquid nitrogen, and diagnosed as nonalcoholic steatohepatitis by histology.

### Statistic Analysis

Student t test is used for data analysis. Bars represent  $\pm$ SD, and asterisks represents  $p < 0.05$  in all corresponding figures.

## SUPPLEMENTAL INFORMATION

Supplemental Information includes Supplemental Experimental Procedures, one table, and five figures and may be found with this article online at doi:10.1016/j.cmet.2010.06.009.

## ACKNOWLEDGMENTS

We thank Drs. E. Mueller, J. Wess, S. Tydlacka, and C. Chisholm for critical reading of the manuscript, and Drs. O. Gavrilova, W. Jou, D. Simon, and C. Li for technical assistance. This work was supported by the intramural Research Program of National Institute of Diabetes, Digestive and Kidney Diseases, National Institutes of Health.

Received: December 4, 2009

Revised: April 1, 2010

Accepted: June 3, 2010

Published: September 7, 2010

## REFERENCES

- Ahmed, M.H., and Byrne, C.D. (2009). Current treatment of non-alcoholic fatty liver disease. *Diabetes Obes. Metab.* *11*, 188–195.
- Ahn, B.H., Kim, H.S., Song, S., Lee, I.H., Liu, J., Vassilopoulos, A., Deng, C.X., and Finkel, T. (2008). A role for the mitochondrial deacetylase Sirt3 in regulating energy homeostasis. *Proc. Natl. Acad. Sci. USA* *105*, 14447–14452.
- Blander, G., and Guarente, L. (2004). The Sir2 family of protein deacetylases. *Annu. Rev. Biochem.* *73*, 417–435.
- Brunet, A., Sweeney, L.B., Sturgill, J.F., Chua, K.F., Greer, P.L., Lin, Y., Tran, H., Ross, S.E., Mostoslavsky, R., Cohen, H.Y., et al. (2004). Stress-dependent regulation of FOXO transcription factors by the SIRT1 deacetylase. *Science* *303*, 2011–2015.

- den Boer, M., Voshol, P.J., Kuipers, F., Havekes, L.M., and Romijn, J.A. (2004). Hepatic steatosis: a mediator of the metabolic syndrome. Lessons from animal models. *Arterioscler. Thromb. Vasc. Biol.* **24**, 644–649.
- Deng, C.X. (2009). SIRT1, is it a tumor promoter or tumor suppressor? *Int. J. Biol. Sci.* **5**, 147–152.
- Deng, X.Q., Chen, L.L., and Li, N.X. (2007). The expression of SIRT1 in nonalcoholic fatty liver disease induced by high-fat diet in rats. *Liver Int.* **27**, 708–715.
- Finkel, T., Deng, C.X., and Mostoslavsky, R. (2009). Recent progress in the biology and physiology of sirtuins. *Nature* **460**, 587–591.
- Gonzali, S., Pistelli, L., De Bellis, L., and Alpi, A. (2001). Characterization of two *Arabidopsis thaliana* fructokinases. *Plant Sci.* **160**, 1107–1114.
- Guarente, L., and Kenyon, C. (2000). Genetic pathways that regulate ageing in model organisms. *Nature* **408**, 255–262.
- Haigis, M.C., and Guarente, L.P. (2006). Mammalian sirtuins—emerging roles in physiology, aging, and calorie restriction. *Genes Dev.* **20**, 2913–2921.
- Harada, N., Oda, Z., Hara, Y., Fujinami, K., Okawa, M., Ohbuchi, K., Yonemoto, M., Ikeda, Y., Ohwaki, K., Aragane, K., et al. (2007). Hepatic de novo lipogenesis is present in liver-specific ACC1-deficient mice. *Mol. Cell. Biol.* **27**, 1881–1888.
- Jacobs, K.M., Pennington, J.D., Bisht, K.S., Aykin-Burns, N., Kim, H.S., Mishra, M., Sun, L., Nguyen, P., Ahn, B.H., Leclerc, J., et al. (2008). SIRT3 interacts with the daf-16 homolog FOXO3a in the Mitochondria, as well as increases FOXO3a Dependent Gene expression. *Int. J. Biol. Sci.* **4**, 291–299.
- Jeong, W.I., Osei-Hyiaman, D., Park, O., Liu, J., Batkai, S., Mukhopadhyay, P., Horiguchi, N., Harvey-White, J., Marsicano, G., Lutz, B., et al. (2008). Paracrine activation of hepatic CB1 receptors by stellate cell-derived endocannabinoids mediates alcoholic fatty liver. *Cell Metab.* **7**, 227–235.
- Kanfi, Y., Shalman, R., Peshti, V., Pilosof, S.N., Gozlan, Y.M., Pearson, K.J., Lerrer, B., Moazed, D., Marine, J.C., de Cabo, R., and Cohen, H.Y. (2008). Regulation of SIRT6 protein levels by nutrient availability. *FEBS Lett.* **582**, 543–548.
- Kawahara, T.L., Michishita, E., Adler, A.S., Damian, M., Berber, E., Lin, M., McCord, R.A., Ongaigui, K.C., Boxer, L.D., Chang, H.Y., and Chua, K.F. (2009). SIRT6 links histone H3 lysine 9 deacetylation to NF-kappaB-dependent gene expression and organismal life span. *Cell* **136**, 62–74.
- Kim, H.S., Patel, K., Muldoon-Jacobs, K., Bisht, K.S., Aykin-Burns, N., Pennington, J.D., van der Meer, R., Nguyen, P., Savage, J., Owens, K.M., et al. (2010). SIRT3 is a mitochondria-localized tumor suppressor required for maintenance of mitochondrial integrity and metabolism during stress. *Cancer Cell* **17**, 41–52.
- Lakso, M., Pichel, J.G., Gorman, J.R., Sauer, B., Okamoto, Y., Lee, E., Alt, F.W., and Westphal, H. (1996). Efficient in vivo manipulation of mouse genomic sequences at the zygote stage. *Proc. Natl. Acad. Sci. USA* **93**, 5860–5865.
- Liszt, G., Ford, E., Kurtev, M., and Guarente, L. (2005). Mouse Sir2 homolog SIRT6 is a nuclear ADP-ribosyltransferase. *J. Biol. Chem.* **280**, 21313–21320.
- Liu, Y., Dentin, R., Chen, D., Hedrick, S., Ravnskjaer, K., Schenk, S., Milne, J., Meyers, D.J., Cole, P., Yates, J., 3rd., et al. (2008). A fasting inducible switch modulates gluconeogenesis via activator/coactivator exchange. *Nature* **456**, 269–273.
- Lombard, D.B., Schwer, B., Alt, F.W., and Mostoslavsky, R. (2008). SIRT6 in DNA repair, metabolism and ageing. *J. Intern. Med.* **263**, 128–141.
- Mahishi, L., and Usdin, K. (2006). NF- $\kappa$ B, AP2, Nrf1 and Sp1 regulate the fragile X-related gene 2 (FXR2). *Biochem. J.* **400**, 327–335.
- Mantel, C., and Broxmeyer, H.E. (2008). Sirtuin 1, stem cells, aging, and stem cell aging. *Curr. Opin. Hematol.* **15**, 326–331.
- Michishita, E., McCord, R.A., Berber, E., Kioi, M., Padilla-Nash, H., Damian, M., Cheung, P., Kusumoto, R., Kawahara, T.L., Barrett, J.C., et al. (2008). SIRT6 is a histone H3 lysine 9 deacetylase that modulates telomeric chromatin. *Nature* **452**, 492–496.
- Michishita, E., McCord, R.A., Boxer, L.D., Barber, M.F., Hong, T., Gozani, O., and Chua, K.F. (2009). Cell cycle-dependent deacetylation of telomeric histone H3 lysine K56 by human SIRT6. *Cell Cycle* **8**, 2664–2666.
- Mostoslavsky, R., Chua, K.F., Lombard, D.B., Pang, W.W., Fischer, M.R., Gellon, L., Liu, P., Mostoslavsky, G., Franco, S., Murphy, M.M., et al. (2006). Genomic instability and aging-like phenotype in the absence of mammalian SIRT6. *Cell* **124**, 315–329.
- Motta, M.C., Divecha, N., Lemieux, M., Kamel, C., Chen, D., Gu, W., Bultsma, Y., McBurney, M., and Guarente, L. (2004). Mammalian SIRT1 represses forkhead transcription factors. *Cell* **116**, 551–563.
- Nemoto, S., Fergusson, M.M., and Finkel, T. (2004). Nutrient availability regulates SIRT1 through a forkhead-dependent pathway. *Science* **306**, 2105–2108.
- Nisoli, E., Tonello, C., Cardile, A., Cozzi, V., Bracale, R., Tedesco, L., Falcone, S., Valerio, A., Cantoni, O., Clementi, E., et al. (2005). Calorie restriction promotes mitochondrial biogenesis by inducing the expression of eNOS. *Science* **310**, 314–317.
- Postic, C., and Girard, J. (2008). Contribution of de novo fatty acid synthesis to hepatic steatosis and insulin resistance: lessons from genetically engineered mice. *J. Clin. Invest.* **118**, 829–838.
- Purushotham, A., Schug, T.T., Xu, Q., Surapureddi, S., Guo, X., and Li, X. (2009). Hepatocyte-specific deletion of SIRT1 alters fatty acid metabolism and results in hepatic steatosis and inflammation. *Cell Metab.* **9**, 327–338.
- Rodgers, J.T., Lerin, C., Haas, W., Gygi, S.P., Spiegelman, B.M., and Puigserver, P. (2005). Nutrient control of glucose homeostasis through a complex of PGC-1 $\alpha$  and SIRT1. *Nature* **434**, 113–118.
- Rodgers, J.T., and Puigserver, P. (2007). Fasting-dependent glucose and lipid metabolic response through hepatic sirtuin 1. *Proc. Natl. Acad. Sci. USA* **104**, 12861–12866.
- Rogers, C.Q., Ajmo, J.M., and You, M. (2008). Adiponectin and alcoholic fatty liver disease. *IUBMB Life* **60**, 790–797.
- Saunders, L.R., and Verdin, E. (2007). Sirtuins: critical regulators at the crossroads between cancer and aging. *Oncogene* **26**, 5489–5504.
- Shindo, Y., Osumi, T., and Hashimoto, T. (1978). Effects of administration of di-(2-ethylhexyl)phthalate on rat liver mitochondria. *Biochem. Pharmacol.* **27**, 2683–2688.
- Tietge, U.J., Bakillah, A., Maugeais, C., Tsukamoto, K., Hussain, M., and Rader, D.J. (1999). Hepatic overexpression of microsomal triglyceride transfer protein (MTP) results in increased in vivo secretion of VLDL triglycerides and apolipoprotein B. *J. Lipid Res.* **40**, 2134–2139.
- Vaquero, A., Scher, M., Erdjument-Bromage, H., Tempst, P., Serrano, L., and Reinberg, D. (2007). SIRT1 regulates the histone methyl-transferase SUV39H1 during heterochromatin formation. *Nature* **450**, 440–444.
- Wang, R.H., Sengupta, K., Li, C., Kim, H.S., Cao, L., Xiao, C., Kim, S., Xu, X., Zheng, Y., Chilton, B., et al. (2008a). Impaired DNA damage response, genome instability, and tumorigenesis in SIRT1 mutant mice. *Cancer Cell* **14**, 312–323.
- Wang, R.H., Zheng, Y., Kim, H.S., Xu, X., Cao, L., Luhasen, T., Lee, M.H., Xiao, C., Vassilopoulos, A., Chen, W., et al. (2008b). Interplay among BRCA1, SIRT1, and Survivin during BRCA1-associated tumorigenesis. *Mol. Cell* **32**, 11–20.
- Xu, X., Li, C., Garrett-Beal, L., Larson, D., Wynshaw-Boris, A., and Deng, C.X. (2001). Direct removal in the mouse of a floxed neo gene from a three-loxP conditional knockout allele by two novel approaches. *Genesis* **30**, 1–6.
- Yakar, S., Liu, J.L., Stannard, B., Butler, A., Accili, D., Sauer, B., and LeRoith, D. (1999). Normal growth and development in the absence of hepatic insulin-like growth factor I. *Proc. Natl. Acad. Sci. USA* **96**, 7324–7329.
- Yang, B., Zwaans, B.M., Eckersdorff, M., and Lombard, D.B. (2009). The sirtuin SIRT6 deacetylates H3 K56Ac in vivo to promote genomic stability. *Cell Cycle* **8**, 2662–2663.
- You, M., Matsumoto, M., Pacold, C.M., Cho, W.K., and Crabbe, D.W. (2004). The role of AMP-activated protein kinase in the action of ethanol in the liver. *Gastroenterology* **127**, 1798–1808.
- Zhong, L., D'Urso, A., Toiber, D., Sebastian, C., Henry, R.E., Vadysirisack, D.D., Guimaraes, A., Marinelli, B., Wikstrom, J.D., Nir, T., et al. (2010). The histone deacetylase Sirt6 regulates glucose homeostasis via Hif1 $\alpha$ . *Cell* **140**, 280–293.